Controlling and Measuring Quantum Transport of Heat in Trapped-Ion Crystals

A. Bermudez, M. Bruderer, and M. B. Plenio

Institut für Theoretische Physik, Albert-Einstein-Allee 11, Universität Ulm, 89069 Ulm, Germany
Center for Integrated Quantum Science and Technology, Albert-Einstein-Allee 11, Universität Ulm, 89069 Ulm, Germany
(Received 12 April 2013; published 22 July 2013)

Measuring heat flow through nanoscale devices poses formidable practical difficulties as there is no "ampere meter" for heat. We propose to overcome this problem in a chain of trapped ions, where laser cooling the chain edges to different temperatures induces a heat current of local vibrations (vibrons). We show how to efficiently control and measure this current, including fluctuations, by coupling vibrons to internal ion states. This demonstrates that ion crystals provide an ideal platform for studying quantum transport, e.g., through thermal analogues of quantum wires and quantum dots. Notably, ion crystals may give access to measurements of the elusive bosonic fluctuations in heat currents and the onset of Fourier's law. Our results are strongly supported by numerical simulations for a realistic implementation with specific ions and system parameters.

DOI: 10.1103/PhysRevLett.111.040601 PACS numbers: 05.60.Gg, 32.80.Qk, 37.10.Ty, 67.85.−d

In view of the rapid development of nanoscale technologies [1], understanding charge and heat transport at the microscopic level has become a central topic of current research. As already shown for fermions [2], charge transport at the nanoscale is typically governed by quantum effects. Transport of heat by bosons, e.g., phonons, is expected to have analogous properties [3]. Thermal experiments, however, are considerably more challenging as there is no device capable of measuring local heat currents [3]. Moreover, heat reservoirs and temperature probes required to study heat transport usually entail spurious interface effects. Within these restrictions, most experimental efforts have focused on detecting temperature profiles [4] in different devices [1,5,6].

In this Letter, we show that trapped-ion crystals are promising platforms for thermal experiments overcoming these limitations. We introduce a quantum transport toolbox containing all functionalities required for treating heat currents on the same footing as electrical currents. By exploiting laser-induced couplings between transverse quantized vibrations (vibrons) and internal degrees of freedom (spins) of the ions, we show how to control and measure heat currents across ion chains [Fig. 1(a)]. Specifically, ions at the edges of the crystal are Doppler cooled to different vibron numbers, equivalent to different temperatures. The edge ions act as unbalanced thermal reservoirs sustaining a heat flow in the form of vibron hopping through the bulk [Fig. 1(b)]. For probing vibron numbers and heat currents (including fluctuations), we map their values onto the spins, which can be measured via spin-dependent fluorescence [7]. We note that thermal experiments with ions are a topic of increasing interest: Propagation of vibrational excitations has been assessed in Ref. [8], while the use of single ions as heat engines has been proposed in Ref. [9]. More relevant to the topic of this work, the thermalization of sympathetically cooled chains has been studied in Ref. [10] by Langevin dynamics [11]. Our toolbox, which is based on thorough first-principles derivations, will be useful for the development of experiments about nonequilibrium statistical mechanics in the quantum regime with trapped ions.

We demonstrate the versatility of this toolbox by the examples of a thermal quantum wire (TQW) and a thermal quantum dot (TQD). We first study the onset of temperature gradients across the TQW according to Fourier's law [12]. This requires the transition from ballistic to diffusive transport, which we induce by (i) dephasing through noisy modulations of the trap frequencies [13] or (ii) disorder in the ion crystal due to engineered spin-vibron couplings [14]. The TQD highlights the differences between bosonic and fermionic transport [15], captured by the statistics of the fluctuations in the heat current [16]. Building on laser-assisted tunneling [17,18], we show how to measure current fluctuations. Moreover, the TQD can be operated as a switch for heat currents, a first step toward a single-spin heat transistor.

Model.—We consider a linear Coulomb crystal with three types of ions [Fig. 1(a)]. Unlike in phonon-mediated quantum computing [19], we focus on vibrons: the quanta of individual transverse oscillations responsible for a local electric dipole. As demonstrated experimentally [20], the interaction between these dipoles leads to a tight-binding model ($\hbar = 1$)

$$H_{\rm tb} = \sum_{\alpha, i_\alpha} \omega_{i_\alpha} a_{i_\alpha}^\dagger a_{i_\alpha} + \sum_{\alpha,\beta} \sum_{i_\alpha \neq j_\beta} (J_{i_\alpha j_\beta} a_{i_\alpha}^\dagger a_{j_\beta} + \text{H.c.}), \tag{1}$$

where the bosonic operators $a_{i_\alpha}^\dagger (a_{i_\alpha})$ create (annihilate) local vibrons, latin indices label lattice sites $i,\ j \in \{1 \cdots N\}$, and greek subindices label species $\alpha,\ \beta \in \{\sigma, \tau, \kappa\}$ [Fig. 1(a)]. The trapping and dipole-dipole couplings yield the on-site energies ω_{i_α} and long-range tunnelings $J_{i_\alpha j_\beta}$. The ion crystal is a natural playground for

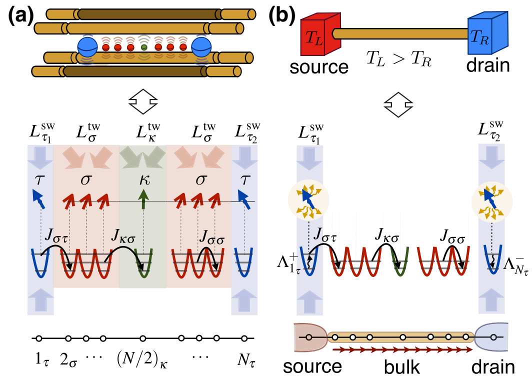

FIG. 1 (color online). Heat transport toolbox: (a) (top) A mixed-species ion crystal in a linear Paul trap (similarly for surface trap arrays). (bottom) Spins and vibrons are indicated by arrows and wells, respectively. Laser arrangements L_τ^{sw} ($L_\sigma^{\mathrm{tw}}, L_\kappa^{\mathrm{tw}}$) control the incoherent (coherent) vibrational dynamics of the ions, with $J_{\alpha\beta}$ the vibron tunneling. (b) (top) A TQW connected to two reservoirs at different temperatures. (bottom) Strong laser cooling with strengths $\Lambda_{\ell_\tau}^- > \Lambda_{\ell_\tau}^+$ allows us to treat τ ions as heat reservoirs, whereas bulk ions σ, κ act as the TQW.

bosonic lattice models [21], where vibrons correspond to bosonic particles, hopping between different lattice sites, and the lattice is determined by the underlying crystal structure. Additionally, we exploit two atomic levels of each ion, denoted as spins $|s_{i_\alpha}\rangle \in \{|\uparrow_{i_\alpha}\rangle, |\downarrow_{i_\alpha}\rangle\}$, with the Hamiltonian $H_s^\alpha = (1/2)\sum_{i_\alpha}\omega_0^\alpha \sigma_{i_\alpha}^z$ and $\sigma_{i_\alpha}^z = |\uparrow_{i_\alpha}\rangle\langle\uparrow_{i_\alpha}| - |\downarrow_{i_\alpha}\rangle\langle\downarrow_{i_\alpha}|$. The atomic transitions are characterized by their frequency ω_0^α and linewidth $\Gamma_\alpha^{\mathrm{eff}}$.

We supplement the dynamics of the vibrons by incoherent and coherent laser-induced processes which are necessary to develop the tools for studying quantum transport.

(i) For incoherent dynamics, we employ a laser forming a standing wave along the vibron direction. This drives dipole-allowed transitions of the α spins and simultaneously increases or decreases the corresponding vibron number. For fast decaying spins, the two processes yield an effective vibron dissipation

$$\mathcal{D}_v^{i_\alpha}(\mu) = \mathcal{D}[\Lambda_{i_\alpha}^+, a_{i_\alpha}^\dagger, a_{i_\alpha}](\mu) + \mathcal{D}[\Lambda_{i_\alpha}^-, a_{i_\alpha}, a_{i_\alpha}^\dagger](\mu), \quad (2)$$

where $\mathcal{D}[\Lambda, O_1, O_2](\bullet) = \Lambda(O_1 \bullet O_2 - O_2 O_1 \bullet) + \mathrm{H.c.}$ is a superoperator acting on the density matrix μ. The local heating (cooling) strength $\Lambda_{i_\alpha}^+$ ($\Lambda_{i_\alpha}^-$) depends on the spectral functions of the couplings [22] and is controlled by the laser parameters [23].

(ii) For coherent dynamics, we apply a spin-dependent traveling wave consisting of two noncopropagating laser beams. The spin-vibron couplings originate from two-photon processes [29], whereby the spin is virtually excited by absorption (emission) of a photon from (into) a different laser beam

$$H_{\mathrm{sv}}^{i_\alpha}(t) = (1/2)(\Delta\omega_\alpha^+ + \Delta\omega_\alpha^- \sigma_{i_\alpha}^z)\cos(\nu_\alpha t - \varphi_\alpha) a_{i_\alpha}^\dagger a_{i_\alpha}, \quad (3)$$

where $\Delta\omega_\alpha^\pm$, ν_α, φ_α are fully controllable.

Equations (1)–(3) form our Liouvillian heat transport toolbox, the driven dissipative spin-vibron model

$$\mathcal{L}_{\mathrm{ddsv}}(\mu) = -i\Big[H_{\mathrm{tb}} + \sum_{\alpha, i_\alpha \in \mathfrak{C}} H_{\mathrm{sv}}^{i_\alpha}(t), \mu\Big] + \sum_{\alpha, i_\alpha \in \mathfrak{I}} \mathcal{D}_{\mathrm{v}}^{i_\alpha}(\mu), \quad (4)$$

where the sets $\mathfrak{C}$, $\mathfrak{I}$ comprise ions subjected to coherent or incoherent effects. We avoid single-ion laser addressing by employing different species for each functionality, such as the implementation of thermal reservoirs. Ideally, these are capable of supplying or absorbing vibrons without changing their state. This is achieved by using a red-detuned laser, such that the cooling (2) with a rate $\gamma_{i_\alpha} = \mathrm{Re}\{(\Lambda_{i_\alpha}^-)^* - \Lambda_{i_\alpha}^+\}$ dominates over the tunneling $\gamma_{i_\alpha} \gg J_{i_\alpha, j_\beta}$ (i.e., the strong-cooling limit) [31]. Thus, the ions remain in a thermal state, providing an accurate implementation of vibronic reservoirs.

Thermal quantum wire.—For designing a TQW, we choose ion species with $\Gamma_\tau^{\mathrm{eff}} \gg \Gamma_\sigma^{\mathrm{eff}}, \Gamma_\kappa^{\mathrm{eff}}$ and implement dissipation only for the τ ions (i.e., $\sigma, \kappa \in \mathfrak{C}$, $\tau \in \mathfrak{I}$). The τ ions, placed at the edges of the chain, are cooled to mean vibron numbers $\bar{n}_{1_\tau} > \bar{n}_{N_\tau}$, such that they act as vibronic batteries, realising the starting point for many transport studies [32]. The left (right) reservoir constantly supplies (absorbs) vibrons in the attempt to equilibrate with the TQW. If combined, the reservoirs sustain a flow of heat along the TQW [Fig. 1(b)].

We assess how the TQW thermalizes in contact with the reservoirs. In the strong-cooling regime, the edge vibrons can be integrated out to obtain a dissipative spin-vibron model for the reduced density matrix of the bulk $\partial_t \mu_{\mathrm{bulk}} = \mathcal{L}_{\mathrm{ddsv}}^{\mathrm{bulk}}(\mu_{\mathrm{bulk}})$,

$$\mathcal{L}_{\mathrm{ddsv}}^{\mathrm{bulk}}(\bullet) = -i\Big[H_{\mathrm{rtb}} + \sum_{\alpha, i_\alpha \in \mathfrak{C}} H_{\mathrm{sv}}^{i_\alpha}(t), \bullet\Big] + \sum_{\alpha i_\alpha, \beta j_\beta \in \mathfrak{C}} \mathcal{D}_{i_\alpha j_\beta}(\bullet). \quad (5)$$

Here, H_{rtb} is identical to Eq. (1) with renormalized parameters. The dissipator is similar to Eq. (2) but extended to all bulk ions $\mathcal{D}_{i_\alpha j_\beta} = \mathcal{D}[\tilde{\Lambda}_{i_\alpha, j_\beta}^+, a_{i_\alpha}^\dagger, a_{j_\beta}] + \mathcal{D}[\tilde{\Lambda}_{i_\alpha, j_\beta}^-, a_{i_\alpha}, a_{j_\beta}^\dagger]$, where $\tilde{\Lambda}_{i_\alpha, j_\beta}^\pm$ depend on the tunneling via the spectral densities $\Gamma_{i_\alpha, j_\beta}^{\ell_\tau} = 2\pi J_{i_\alpha, \ell_\tau} \rho_{\ell_\tau}(\omega_{i_\alpha}) J_{\ell_\tau, j_\beta}$, including the reservoir density of states ρ_{ℓ_τ} [33]. Hence, the bulk-reservoir-bulk tunneling of vibrons introduces an effective dissipation responsible for the thermalization of the TQW.

The dipolar decay of tunneling with distance suggests that vibron exchange with bulk ions adjacent to the reservoirs dominates thermalization. In the strong-cooling regime, we thus predict a homogeneous steady-state vibron occupation

$$\langle n_{i_\alpha}\rangle_{\mathrm{ss}} = \frac{\Gamma_L \bar{n}_L + \Gamma_R \bar{n}_R}{\Gamma_L + \Gamma_R}, \quad \alpha, i_\alpha \in \mathfrak{C}, \quad (6)$$

with the local couplings $\Gamma_L = \Gamma^{1_\tau}_{2_\sigma,2_\sigma}$, $\Gamma_R = \Gamma^{N_\tau}_{(N-1)_\sigma,(N-1)_\sigma}$ and the reservoir mean occupations $\bar{n}_L = \bar{n}_{1_\tau}$, $\bar{n}_R = \bar{n}_{N_\tau}$. Similar arguments apply to the vibron current, defined through $\partial_t n_{i_\alpha} = I^{\rm vib}_{\rightarrow i_\alpha} - I^{\rm vib}_{i_\alpha \rightarrow}$, which is independent of the TQW length

$$\langle I^{\rm vib}_{i_\alpha \rightarrow}\rangle_{\rm ss} = \langle I^{\rm vib}_{\rightarrow i_\alpha}\rangle_{\rm ss} = \frac{\Gamma_L \Gamma_R}{\Gamma_L + \Gamma_R}(\bar{n}_L - \bar{n}_R), \quad \alpha, i_\alpha \in \mathfrak{C}. \tag{7}$$

Numerical solutions of the complete dissipative dynamics in Eq. (5) fully confirm these predictions [31]. Our results are different from Fourier's law of thermal conduction [12], which predicts (i) a linear temperature gradient, i.e., $\langle n_{i_\alpha}\rangle_{\rm FL} = \bar{n}_L + (\bar{n}_R - \bar{n}_L) i_\alpha / N$; and (ii) a heat current inversely proportional to the length of the wire $\langle I^{\rm vib}_{i_\alpha \rightarrow}\rangle_{\rm FL} \propto (\bar{n}_L - \bar{n}_R)/N$. The disagreement is expected since Fourier's law applies to diffusive processes; in contrast, Eqs. (6) and (7) describe ballistic transport of vibrons, analogous to ballistic electronic transport [34].

We now consider two phase-breaking processes resulting in a ballistic-diffusive crossover: dephasing [35] and disorder [36]. Dephasing can be engineered by modulating trap frequencies with a noisy voltage [13]. We model such noise as dynamic fluctuations of the on-site energies in Eq. (1), $\omega_{i_\alpha} \rightarrow \omega_{i_\alpha} + \delta\omega_{i_\alpha}(t)$, with $\delta\omega_{i_\alpha}(t)$ a random process. In a Born-Markov approximation, this leads to an additional term in Eq. (4), $\mathcal{L}_{\rm ddsv} \rightarrow \mathcal{L}_{\rm ddsv} + \mathcal{D}_d$, where

$$\mathcal{D}_d(\bullet) = \sum_{\alpha,\beta} \sum_{i_\alpha, j_\beta} \Gamma_d e^{-[(|\mathbf{r}^0_{i_\alpha} - \mathbf{r}^0_{j_\beta}|)/\xi_c]} (n_{i_\alpha} \bullet n_{j_\beta} - n_{j_\beta} n_{i_\alpha} \bullet) + \text{H.c.},$$

with the dephasing rate Γ_d and the noise correlation length ξ_c [37]. Figure 2(a) shows homogeneous vibron distributions along the TQW without dephasing. For dephasing with $\xi_c \ll L$, we observe the onset of a linear gradient along the microtrap array [Fig. 2(b), left], pinpointing diffusive transport. For the linear Paul trap, the inhomogeneous crystal modifies the gradient, yielding an anomalous Fourier's law [Fig. 2(b), right].

Disorder can be modeled by modifying the on-site energies of Eq. (1), $\omega_{i_\alpha} \rightarrow \omega_{i_\alpha} + \Delta\omega_\alpha$, with $\Delta\omega_\alpha$ a static random variable. To obtain such disorder, we apply a strong static spin-vibron coupling (3) with parameters $\nu_\alpha = 0$, $\varphi_\alpha = 0$, $\Delta\omega^+_\alpha = 0$, and $\Delta\omega^-_\alpha \neq 0$, such that the vibrons experience a spin-dependent inhomogeneous landscape of on-site energies, resulting in vibron scattering [14]. With each bulk spin initialized in $|+_{i_\alpha}\rangle = (|\uparrow_{i_\alpha}\rangle + |\downarrow_{i_\alpha}\rangle)/\sqrt{2}$, the tight-binding model becomes stochastic $H_{\rm tb} \rightarrow H_{\rm stb} = \sum_{\alpha, i_\alpha} \epsilon_{i_\alpha} a^\dagger_{i_\alpha} a_{i_\alpha} + \sum_{\alpha,\beta} \sum_{i_\alpha \neq j_\beta} J_{i_\alpha j_\beta} a^\dagger_{i_\alpha} a_{j_\beta} +$ H.c. Here, the on-site energies are binary random variables sampling $\epsilon_{i_\alpha} \in \{\omega_\alpha - (1/2)\Delta\omega^-_\alpha, \omega_\alpha + (1/2)\Delta\omega^-_\alpha\}$ with probabilities $p(\epsilon_{i_\alpha}) = 1/2$ inherited from the quantum parallelism. This randomness leads to Anderson localization, whereby normal modes display a finite localization length $\xi_{\rm loc}$ [38]. For the small ion crystals of length L, the modes with $\xi_{\rm loc} \gg L$ contribute ballistically, those with $\xi_{\rm loc} \lesssim L$ introduce diffusion, and those with $\xi_{\rm loc} \ll L$ do not contribute to transport. We thus expect that the heat transport is much richer in the disordered case. Figure 2(c) shows the disorder-averaged distribution of vibron occupations along the TQW, where we find clear anomalies in Fourier's law, measurable in experiments.

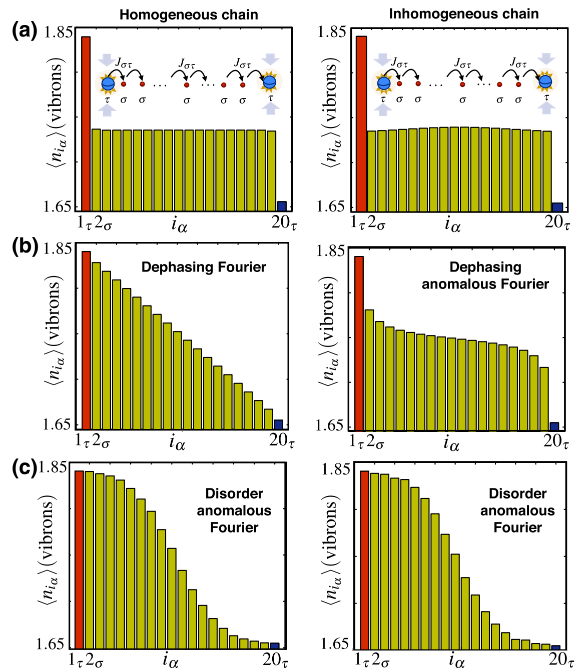

FIG. 2 (color online). Fourier's law: Vibron distribution in the steady state of a chain with $N = 20$ ions (left: microtrap array, right: linear Paul trap). (a) Ballistic regime (agreeing with Ref. [10]), (b) the dephasing-induced diffusive regime, and (c) the disorder-induced diffusive regime.

To distinguish ballistic from diffusive transport, we suggest a measuring scheme inspired by Refs. [39,40]. We map the mean value of any vibron operator $\langle O_{i_\alpha}\rangle_{\rm ss}$ and its fluctuation spectrum

$$S_{O_{i_\alpha} O_{i_\alpha}}(\omega) = \int_0^\infty dt \langle \tilde{O}_{i_\alpha}(t) \tilde{O}_{i_\alpha}(0)\rangle_{\rm ss} e^{-i\omega t},$$
$$\tilde{O}_{i_\alpha} = O_{i_\alpha} - \langle O_{i_\alpha}\rangle_{\rm ss}$$

onto the spin coherences, while disturbing the vibron states minimally. This is achieved through Ramsey-type interferometry based on engineered spin-vibron interactions $\tilde{H}^O_{\rm sv} = \sum_{i_\kappa} (1/2)\lambda_O O_{i_\kappa} \sigma^z_{i_\kappa}$, with weak coupling λ_O [31].

A single κ ion [41] initialized in the state $|+_{i_\kappa}\rangle$ by a $\pi/2$ pulse acquires phase information about the steady-state vibron observable. We perform another $\pi/2$ pulse and measure the probability of observing the state $|\downarrow_{i_\kappa}\rangle$, which is equivalent to measuring the spin coherences

$$\langle \tilde{\sigma}^x_{i_\kappa}(t)\rangle = \cos(\lambda_O \langle O_{i_\kappa}\rangle_{\rm ss} t) e^{-\lambda_O^2 {\rm Re}\{S_{O_{i_\kappa} O_{i_\kappa}}(0)\} t}. \tag{8}$$

Therefore, the period (decay) of the spin oscillations yields the mean value (zero-frequency fluctuations) of the vibron operator $\langle O_{i_\kappa}\rangle_{\rm ss}$ $[S_{O_{i_\kappa}O_{i_\kappa}}(0)]$. Considering the excellent accuracies achieved in projective spin measurements [42], probing steady-state vibrons with this method promises to be very efficient. For measuring the mean vibron number $O_{i_\kappa} = n_{i_\kappa}$, we choose a weak static spin-vibron coupling (3) with $\nu_\kappa = 0$, $\varphi_\kappa = 0$, $\Delta\omega_\kappa^+ = 0$, and $\Delta\omega_\kappa^- \neq 0$. Similarly, vibron density-density correlators can be probed by using several κ ions.

Thermal quantum dot and single-spin heat switch.—The TQD is formed by a single κ ion at position p_κ in the center of the bulk. We use the remaining σ ions as thermal contacts by employing a strong static spin-phonon coupling (3) with parameters $\nu_\sigma = 0$, $\varphi_\sigma = 0$, $\Delta\omega_\sigma^+ = 0$, and $\Delta\omega_\sigma^- \neq 0$. If the spins are initialized in $|\psi_0\rangle = |\downarrow_\sigma\cdots\downarrow_\sigma\rangle|\phi_\kappa\rangle|\uparrow_\sigma\cdots\uparrow_\sigma\rangle$, there is a large shift of the on-site energies across p_κ, inhibiting tunneling through the TQD. The two halves of the chain thus thermalize independently, i.e., $\langle n_{i_\sigma}\rangle_{\rm ss} = \bar{n}_L$ for $i_\sigma < p_\kappa$ and $\langle n_{i_\sigma}\rangle_{\rm ss} = \bar{n}_R$ for $i_\sigma > p_\kappa$, functioning as thermal leads connected to the quantum dot. The Liouvillian is $\mathcal{L}_{\rm ddtb}^{\rm bulk} = \mathcal{L}_L + \mathcal{L}_{L\kappa R} + \mathcal{L}_R$, where $\mathcal{L}_{L/R}$ describe the uncoupled halves (5) and $\mathcal{L}_{L\kappa R}$ describes the TQD. Transport through the TQD is achieved by using a dynamical spin-vibron coupling (3) for the κ ion. For spin-independent drivings $\Delta\omega_\kappa^- = 0$, the periodic modulation of the on-site energies results in photon-assisted tunneling, overcoming the on-site energy gradient between the dot and the leads [18]. We exploit the spin dependence of this driving to build a single-spin heat switch and a current probe.

For the single-spin heat switch, the parameters of the spin-vibron coupling (3) are $\nu_\kappa = (1/2)\Delta\omega_\sigma^-$, $\varphi_\kappa = 0$, and $\Delta\omega_\kappa^- = \Delta\omega_\kappa^+$, which lead to $\mathcal{L}_{L\kappa R}(\bullet) = -i[H_{L\kappa R}^{\rm PAT}, \bullet] + \mathcal{D}_{p_\kappa p_\kappa}(\bullet)$, where

$$H_{L\kappa R}^{\rm PAT} = -\sum_{i_\sigma < p_\kappa} J_{p_\kappa i_\sigma}^{\rm PAT}(\sigma_{p_\kappa}^z) a_{p_\kappa}^\dagger a_{i_\sigma} + \sum_{i_\sigma > p_\kappa} J_{p_\kappa i_\sigma}^{\rm PAT}(\sigma_{p_\kappa}^z) a_{p_\kappa}^\dagger a_{i_\sigma} + \text{H.c.}$$

The tunneling is spin dependent, i.e., $J_{p_\kappa i_\sigma}^{\rm PAT}(\sigma_{p_\kappa}^z)|\downarrow_{p_\kappa}\rangle = 0$ and $J_{p_\kappa i_\sigma}^{\rm PAT}(\sigma_{p_\kappa}^z)|\uparrow_{p_\kappa}\rangle \neq 0$, because of the operator argument in the first Bessel function $J_{p_\kappa i_\sigma}^{\rm PAT}(\sigma_{p_\kappa}^z) = \tilde{J}_{p_\kappa i_\sigma}\mathfrak{J}_1[\zeta_\kappa(1 + \sigma_{p_\kappa}^z)]$, with $\zeta_\kappa = \Delta\omega_\kappa^+/2\nu_\kappa$ [31]. Therefore, by controlling the κ-spin state via microwave π pulses, we can switch on and off the heat current through the TQD. Different switches have been studied in Ref. [43] to control the entanglement in harmonic chains.

Probing vibron currents requires a minimally perturbing mapping of the current onto the κ spin. This requires a bichromatic spin-vibron coupling (3) with specific parameters [44]. The first frequency induces photon-assisted tunneling

$$H_{L\kappa R}^{\rm PAT} = \sum_{i_\sigma} (\tilde{J}_{i_\sigma, p_\kappa}^{\rm PAT} a_{i_\sigma}^\dagger a_{p_\kappa} + \text{H.c.}), \quad \tilde{J}_{i_\sigma, p_\kappa}^{\rm PAT} = -i2\tilde{J}_{i_\sigma p_\kappa}\mathfrak{J}_1(\pi),$$

such that the tunneling amplitude becomes purely imaginary. This is crucial to devise the probe since the second frequency leads to the necessary spin-current interactions $H_{\rm sv}^I = (1/2)\tilde{\lambda}_I I_{p_k}^{\rm vib}\sigma_{p_k}^z$, where $I_{p_k} = (1/2)(I_{p_k\rightarrow}^{\rm vib} + I_{\rightarrow p_k}^{\rm vib})$. In the limit $\zeta_{k,2} \to 0$, $\tilde{\lambda}_I \approx 4\zeta_{k,2}/\pi$, we get a Ramsey probe (8) for the current mean value $\langle I_{p_k}^{\rm vib}\rangle$ and fluctuations $S_{I_{p_k}^{\rm vib} I_{p_k}^{\rm vib}}(0)$.

Measuring fluctuations is essential for comparing fermionic and bosonic currents via the Fano factor $\mathcal{F} = S_{I_{p_k}^{\rm vib} I_{p_k}^{\rm vib}}(0)/2\langle I_{p_k}^{\rm vib}\rangle$. For heat currents through a symmetrically coupled TQD, we expect strong super-Poissonian fluctuations $\mathcal{F} \gg 1$, which increase linearly with $\bar{n}_L$ in the regime $\bar{n}_L \gg \bar{n}_R$ [16,45]. Unlike the sub-Poissonian fluctuations $\mathcal{F} < 1$ in electrical currents, super-Poissonian fluctuations in heat currents have not been observed yet.

Conclusions.—We have outlined the implementation of an ion-trap toolbox for quantum heat transport, which provides (i) thermal reservoirs, quantum dots, and wires, (ii) engineered on-site disorder and dephasing, and (iii) noninvasive probes for vibron occupations and currents. It would be of the utmost interest to assess the validity of the proposed probes for capturing the full counting statistics of heat transport. All these functionalities significantly extend the possible range of experiments on heat transport. Laser-cooled edge ions in coherent or squeezed vibron states [46] may constitute valuable supplementary gadgets. We expect, moreover, interesting effects in the presence of nonlinearities, e.g., the interplay with Mott insulators [21], competition between dephasing and interactions [47], thermal rectification [48], and structural phase transitions [49]. In a nonequilibrium version of the spin-Peierls instability [50], correlations between structural change and heat currents may be explored.

A. B., M. B., and M. B. P. are supported by PICC and the Alexander von Humboldt Foundation. A. B. thanks FIS2009-10061, QUITEMAD.

[1] D. G. Cahill, W. K. Ford, K. E. Goodson, G. D. Mahan, A. Majumdar, H. J. Maris, R. Merli, and S. R. Phillpot, J. Appl. Phys. **93**, 793 (2003); E. Pop, Nano Res. **3**, 147 (2010).

[2] S. Gustavsson, R. Leturcq, M. Studer, I. Shorubalko, T. Ihn, K. Ensslin, D. C. Driscoll, and A. C. Gossard, Surf. Sci. Rep. **64**, 191 (2009); N. A. Zimbovskaya and M. R. Pederson, Phys. Rep. **509**, 1 (2011).

[3] Y. Dubi and M. Di Ventra, Rev. Mod. Phys. **83**, 131 (2011).

[4] A. Majumdar, Annu. Rev. Mater. Sci. **29**, 505 (1999).

[5] P. Kim, L. Shi, A. Majumdar, and P. L. McEuen, Phys. Rev. Lett. **87**, 215502 (2001); R. Chen, A. I. Hochbaum, P. Murphy, J. Moore, P. Yang, and A. Majumdar, Phys. Rev. Lett. **101**, 105501 (2008); J. H. Seol, I. Jo, A. L. Moore, L. Lindsay, Z. H. Aitken, M. T. Pettes, X. Li, Z. Yao, R. Huang, D. Broido, N. Mingo, R. S. Ruoff, and L. Shi, Science **328**, 213 (2010).

[6] K. Schwab, E. A. Henriksen, J. M. Worlock, and M. L. Roukes, Nature (London) **404**, 974 (2000).

[7] D. J. Wineland, C. Monroe, W. M. Itano, D. Leibfried, B. E. King, and D. M. Meekhof, J. Res. Natl. Inst. Stand. Technol. **103**, 259 (1998).

[8] T. Pruttivarasin, M. Ramm, I. Talukdar, A. Kreuter, and H. Häffner, New J. Phys. **13**, 075012 (2011).

[9] O. Abah, J. Rossnagel, G. Jacob, S. Deffner, F. Schmidt-Kaler, K. Singer, and E. Lutz, Phys. Rev. Lett. **109**, 203006 (2012).

[10] G.-D. Lin and L.-M. Duan, New J. Phys. **13**, 075015 (2011).

[11] U. Zürcher and P. Talkner, Phys. Rev. A **42**, 3267 (1990); **42**, 3278 (1990).

[12] See S. Lepri, R. Livi, and A. Politi, Phys. Rep. **377**, 1 (2003) and references therein.

[13] C. J. Myatt, B. E. King, Q. A. Turchette, C. A. Sackett, D. Kielpinski, W. M. Itano, C. Monroe, and D. J. Wineland, Nature (London) **403**, 269 (2000).

[14] A. Bermudez, M. A. Martin-Delgado, and D. Porras, New J. Phys. **12**, 123016 (2010).

[15] M. Esposito, U. Harbola, and S. Mukamel, Rev. Mod. Phys. **81**, 1665 (2009).

[16] U. Harbola, M. Esposito, and S. Mukamel, Phys. Rev. B **76**, 085408 (2007).

[17] D. H. Dunlap and V. M. Kenkre, Phys. Rev. B **34**, 3625 (1986); F. Grossmann, T. Dittrich, P. Jung, and P. Hänggi, Phys. Rev. Lett. **67**, 516 (1991); M. Holthaus, Phys. Rev. Lett. **69**, 351 (1992).

[18] A. Bermudez, T. Schaetz, and D. Porras, Phys. Rev. Lett. **107**, 150501 (2011); New J. Phys. **14**, 053049 (2012).

[19] T. D. Ladd, F. Jelezko, R. Laflamme, Y. Nakamura, C. Monroe, and J. L. OBrien, Nature (London) **464**, 45 (2010).

[20] K. R. Brown, C. Ospelkaus, Y. Colombe, A. C. Wilson, D. Leibfried, and D. J. Wineland, Nature (London) **471**, 196 (2011); M. Harlander, R. Lechner, M. Brownnutt, R. Blatt, and W. Hänsel, Nature (London) **471**, 200 (2011); S. Haze, Y. Tateishi, A. Noguchi, K. Toyoda, and S. Urabe, Phys. Rev. A **85**, 031401(R) (2012).

[21] D. Porras and J. I. Cirac, Phys. Rev. Lett. **93**, 263602 (2004).

[22] J. I. Cirac, R. Blatt, P. Zoller, and W. D. Phillips, Phys. Rev. A **46**, 2668 (1992).

[23] Note that laser cooling of mixed crystals has been shown for traveling waves [24], and standing-wave cooling may be achieved along the lines of Ref. [25]. Possible alternatives for the required strong cooling are schemes based on the dynamical Stark shift [26], electromagnetic-induced transparency cooling [27], or pulsed sequences [28].

[24] M. D. Barrett, B. DeMarco, T. Schaetz, V. Meyer, D. Leibfried, J. Britton, J. Chiaverini, W. M. Itano, B. Jelenkovic, J. D. Jost, C. Langer, T. Rosenband, and D. J. Wineland, Phys. Rev. A **68**, 042302 (2003); J. P. Home, M. J. McDonnell, D. J. Szwer, B. C. Keitch, D. M. Lucas, D. N. Stacey, and A. M. Steane, Phys. Rev. A **79**, 050305 (R) (2009); J. P. Home, D. Hanneke, J. D. Jost, J. M. Amini, D. Leibfried, and D. J. Wineland, Science **325**, 1227 (2009).

[25] A. Walther, U. Poschinger, K. Singer, and F. Schmidt-Kahler, Appl. Phys. B **107**, 1061 (2012).

[26] A. Retzker and M. B. Plenio, New J. Phys. **9**, 279 (2007).

[27] G. Morigi, J. Eschner, and C. H. Keitel, Phys. Rev. Lett. **85**, 4458 (2000); C. F. Roos, D. Leibfried, A. Mundt, F. Schmidt-Kaler, J. Eschner, and R. Blatt, Phys. Rev. Lett. **85**, 5547 (2000); Y. Lin, J. P. Gaebler, T. R. Tan, R. Bowler, J. D. Jost, D. Leibfried, and D. J. Wineland, Phys. Rev. Lett. **110**, 153002 (2013).

[28] S. Machnes, M. B. Plenio, B. Reznik, A. M. Steane, and A. Retzker, Phys. Rev. Lett. **104**, 183001 (2010).

[29] Note that similar couplings, but linear in the vibron operators, have been demonstrated experimentally [30].

[30] D. Leibfried, B. DeMarco, V. Meyer, D. Lucas, M. Barrett, J. Britton, W. M. Itano, B. Jelenkovic, C. Langer, T. Rosenband, and D. J. Wineland, Nature (London) **422**, 412 (2003); A. Friedenauer, H. Schmitz, J. T. Glueckert, D. Porras, and T. Schaetz, Nat. Phys. **4**, 757 (2008).

[31] See Supplemental Material at http://link.aps.org/supplemental/10.1103/PhysRevLett.111.040601 for a detailed derivation.

[32] K. Saito, Europhys. Lett. **61**, 34 (2003); M. Michel, M. Hartmann, J. Gemmer, and G. T. Mahler, Eur. Phys. J. B **34**, 325 (2003); T. Prosen, New J. Phys. **10**, 043026 (2008).

[33] $\tilde{\Lambda}^{+}_{i_\alpha,j_\beta} = \sum_{\ell_\tau}(1/2)\Gamma^{\ell_\tau}_{i_\alpha,j_\beta}\bar{n}_{\ell_\tau}$ and $\tilde{\Lambda}^{-}_{i_\alpha,j_\beta} = \sum_{\ell_\tau}(1/2)\times \Gamma^{\ell_\tau}_{i_\alpha,j_\beta}(\bar{n}_{\ell_\tau}+1)$ are the nonlocal heating or cooling strengths, expressed in terms of the reservoir density of states $\rho_{\ell_\tau}(\epsilon) = \gamma_{\ell_\tau}/\pi\{[(\epsilon-\delta_{\ell_\tau})-\omega_{\ell_\tau}]^2+\gamma^2_{\ell_\tau}\}$, with $\delta_{\ell_\tau} = \mathrm{Im}\{\Lambda^{+}_{\ell_\tau}-(\Lambda^{-}_{\ell_\tau})^*\}$.

[34] J. C. Cuevas and E. Scheer, *Molecular Electronics: An Introduction to Theory and Experiment* (World Scientific, London, 2010).

[35] Y. Dubi and M. Di Ventra, Phys. Rev. E **79**, 042101 (2009); A. Asadian, D. Manzano, M. Tiersch, and H. J. Briegel, Phys. Rev. E **87**, 012109 (2013).

[36] R. J. Rubin and W. L. Greer, J. Math. Phys. (N.Y.) **12**, 1686 (1971); A. Casher and J. L. Lebowitz, J. Math. Phys. (N.Y.) **12**, 1701 (1971).

[37] The parameter ξ_c may be controlled accurately in microtrap arrays and to some extent in the more standard linear Paul traps.

[38] P. W. Anderson, Phys. Rev. **109**, 1492 (1958).

[39] M. Bruderer and D. Jaksch, New J. Phys. **8**, 87 (2006).

[40] G. B. Lesovik, F. Hassler, and G. Blatter, Phys. Rev. Lett. **96**, 106801 (2006).

[41] Since the coherence of the spins used to introduce disorder is lost due to the strong spin-vibron couplings, we modify the configuration in Fig. 1(a) by introducing a small number of κ ions for measuring while reserving the σ spins for disorder.

[42] H. Haeffner, C. F. Roos, and R. Blatt, Phys. Rep. **469**, 155 (2008).

[43] M. B. Plenio, J. Hartley, and J. Eisert, New J. Phys. **6**, 36 (2004).

[44] The parameters of the bichromatic spin-vibron coupling are $\varphi_{\kappa,1} = \pi/2$, $\varphi_{\kappa,2} = 0$, $\nu_{\kappa,1} = \nu_{\kappa,2} = (1/2)\Delta\omega^{-}_{\sigma}$, and $\Delta\omega^{-}_{\kappa,1} = \Delta\omega^{-}_{\kappa,2} = 0$. $\zeta_{\kappa,1} = \Delta\omega^{+}_{\kappa,1}/2\nu_{\kappa,1} = \pi$ and $\zeta_{\kappa,2} = \Delta\omega^{+}_{\kappa,2}/2\nu_{\kappa,2} \ll 1$.

[45] M. Kindermann, Yu. V. Nazarov, and C. W. J. Beenakker, Phys. Rev. Lett. **88**, 063601 (2002).

[46] J. F. Poyatos, J. I. Cirac, and P. Zoller, Phys. Rev. Lett. **77**, 4728 (1996).

[47] J. J. Mendoza-Arenas, S. Al-Assam, S. R. Clark, and D. Jaksch, arXiv:1303.6353.

[48] D. Segal and A. Nitzan, Phys. Rev. Lett. **94**, 034301 (2005).

[49] S. Fishman, G. De Chiara, T. Calarco, and G. Morigi, Phys. Rev. B **77**, 064111 (2008); A. Retzker, R. C. Thompson, D. M. Segal, and M. B. Plenio, Phys. Rev. Lett. **101**, 260504 (2008).

[50] A. Bermudez and M. B. Plenio, Phys. Rev. Lett. **109**, 010501 (2012).